Electronic Supplementary Information

A Naphthalimide-based Thermometer: heat-induce fluorescent "turn-on" sensing in a wide temperature range in atmosphere

Shuxin Wang, Jian Cao,* and Chenhong Lu

School of Chemistry and Chemical Engineering, Shanghai University of Engineering Science, 333 Longteng Road, Shanghai, 201620, P. R. China Fax: 86-21-67791214

E-mail: caoj@sues.edu.cn

Contents

1. General information

1.1 Materials and Instruments

All reagents and solvents were used as received without further purification. Deionized water was used in the experiments throughout. Silica gel (200-300 mesh) was used for column chromatography. High resolution mass spectra measurements were performed on a LCMS-IT-TOF MS spectrometry. NMR spectra were recorded on a Varian 400 MHz with chemical shifts reported as ppm (in DMSO-*d6* or $CDCl_3$, TMS as internal standard). Fluorescent measurements were performed on a FS-5 spectrophotometer (Edinburgh, Britain) and the slit width was set as 2 nm for excitation and emission, respectively. Absorption spectrum was measured on a SHIMADZU UV-3600 spectrophotometer. Solvents were generally dried and distilled prior to use. The measurements were performed at room temperature on air-equilibrate solutions (10^{-6} M). Dark-Field (DF) microscopy imaging is performed under a Nikon inverted microscope (ECLIPSE Ti−U). In DF mode, the microscope utilizes a Nikon Plan Fluor 100×0.5-1.3 oil iris objective and a Nikon DF condenser.

1.2 Synthesis and Characterization

Synthesis of compound 2

The mixture of N-butyl-4-bromonaphthalimide (3.31 g, 0.01 mol) and 2.85 g formylphenyl piperazine (0.015 mol, 1.5 equiv.) in 5 mL N,N-ethyl-formamide (DMF)

was refluxed under nitrogen atmosphere for 6 h. The TLC technology inspected the reaction degree. The solvent was evaporated under reduced pressure and washed with 20 mL of brine after the completion of the reaction.

After extracted with 75 mL (3×25 mL) dichloromethane and dried with anhydrous sodium sulfate, the crude product was chromatographed using an eluent of petroleum ether : ethyl acetate (5 : 1), which was purified (silica gel, 200 mesh) to yield 2.74 g of a yellow solid powder, a yield of 62%. ^{1}H NMR (400 MHz, CD_3CN) δ 9.87 (s, 1H), 8.64 (dd, *J* = 7.4, 1.2 Hz, 1H), 8.58 (d, *J* = 8.0 Hz, 1H), 8.49 (dd, *J* = 8.5, 1.3 Hz, 1H), 7.82 (d, *J* = 8.9 Hz, 3H), 7.36 (d, *J* = 8.1 Hz, 1H), 7.14 (d, *J* = 8.5 Hz, 2H).4.25 - 4.16 (m, 2H), 3.74 (t, *J* = 5.0 Hz, 4H), 3.45 (t, *J* = 5.0 Hz, 4H), 1.74 (p, *J* = 7.7 Hz, 2H), 1.51 - 1.44 (m, 2H), 1.00 (t, *J* = 7.3 Hz, 3H). ^{13}C NMR (100 MHz, $CDCl_3$) δ 190.36, 164.35, 163.91, 155.10, 154.92, 132.32, 131.84, 131.18, 129.72, 128.02, 126.31, 126.02, 115.20, 114.08, 52.71, 47.64, 40.14, 30.27, 20.38, 13.80. HRMS (ESI) calcd for $C_{27}H_{28}N_3O_3$: 442.2131; found: 442.2124. $[M + H]^+$.

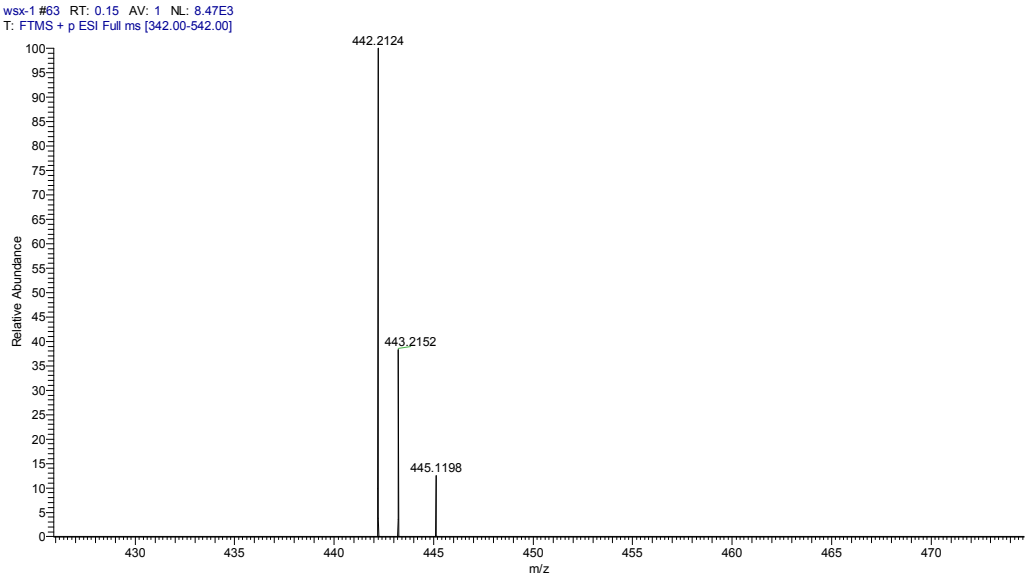

Figure S1 HRMS of compound 2

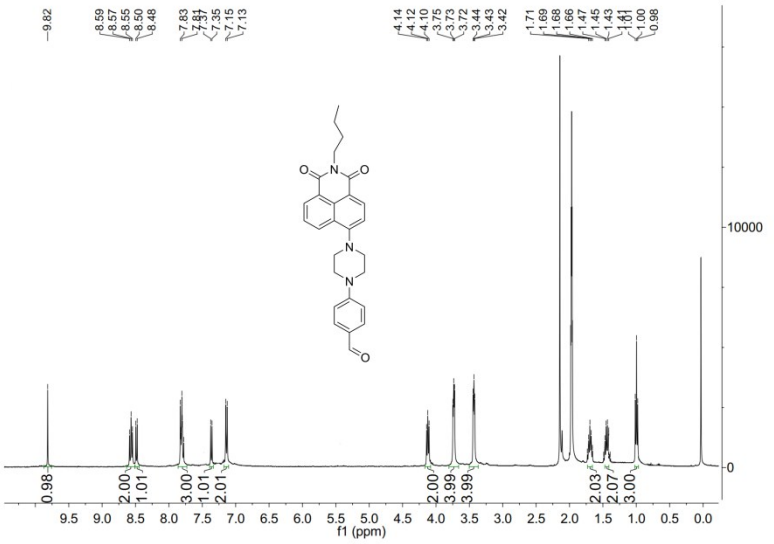

Figure S2 ^{1}H NMR spectrum of compound 2 in CD_3CN

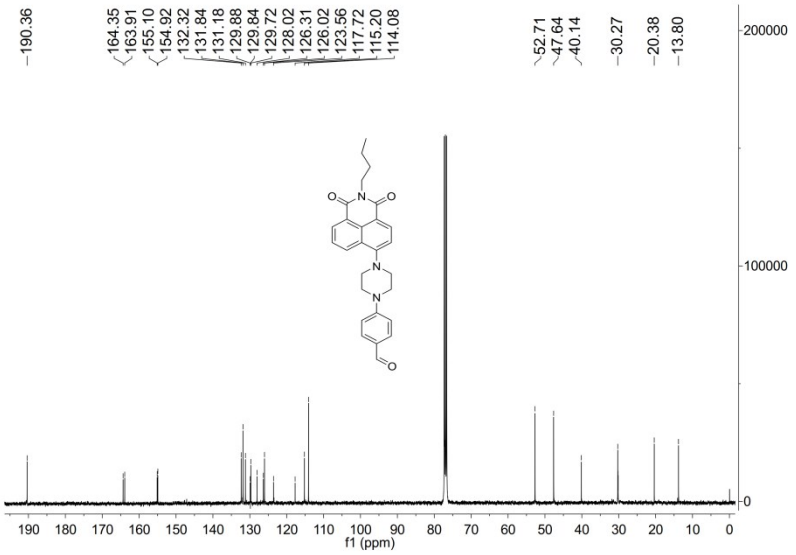

Figure S3 ^{13}C NMR spectrum of compound 2 in $CDCl_3$

Synthesis of Sensor NapPT-1

The mixture of compound 2 (200 mg, 0.45 mmol) and propanethiol (51.6 mg, 0.675 mmol, 1.5 equiv.) in 25 ml dichloromethane was stirred at 0 °C under nitrogen atmosphere for 10 min. 0.04 mL boron trifluoride diethyl ether solution, diluted with

1 mL dichloromethane, was added dropwise to the reaction solution. The solution was continuously stirring for 1 h at the room temperature. Subsequently, the reaction solution was washed with 75 ml (3×25 mL) saturated sodium chloride solution, extracted with methylene chloride, and dried with anhydrous sodium sulfate. The crude product was purified by silica chromatography (PE : EtOAc = 10 : 1, v : v) to afford an yellow solid product (259.29 mg, a yield of 99%). ^{1}H NMR (400 MHz, CD_3CN) δ 8.56 (t, *J* = 7.5 Hz, 2H), 8.49 (d, *J* = 8.1 Hz, 1H), 7.84 - 7.75 (m, 1H), 7.38 (dd, *J* = 8.4, 3.4 Hz, 3H), 7.03 (d, *J* = 8.7 Hz, 2H), 4.97 (s, 1H), 4.16 - 4.07 (m, 2H), 3.55 - 3.47 (m, 4H), 3.46 - 3.40 (m, 4H), 2.54 (dtd, *J* = 20.1, 12.8, 7.3 Hz, 5H), 1.60 (dd, *J* = 14.5, 7.3 Hz, 4H), 1.44 (dd, *J* = 14.5, 7.0 Hz, 3H), 0.98 (dt, *J* = 11.0, 7.3 Hz, 9H). ^{13}C NMR (100 MHz, $CDCl_3$) δ 164.43, 164.00, 155.54, 150.41, 132.43, 132.07, 131.13, 130.08, 129.83, 128.65, 126.22, 125.83, 116.04, 115.04, 53.06, 52.66, 49.32, 40.13, 34.36, 30.28, 22.61, 20.40, 13.86, 13.57. HRMS (ESI) calcd for $C_{33}H_{42}N_3O_2S_2$: 576.2718; found: 576.2709. $[M + H]^+$.

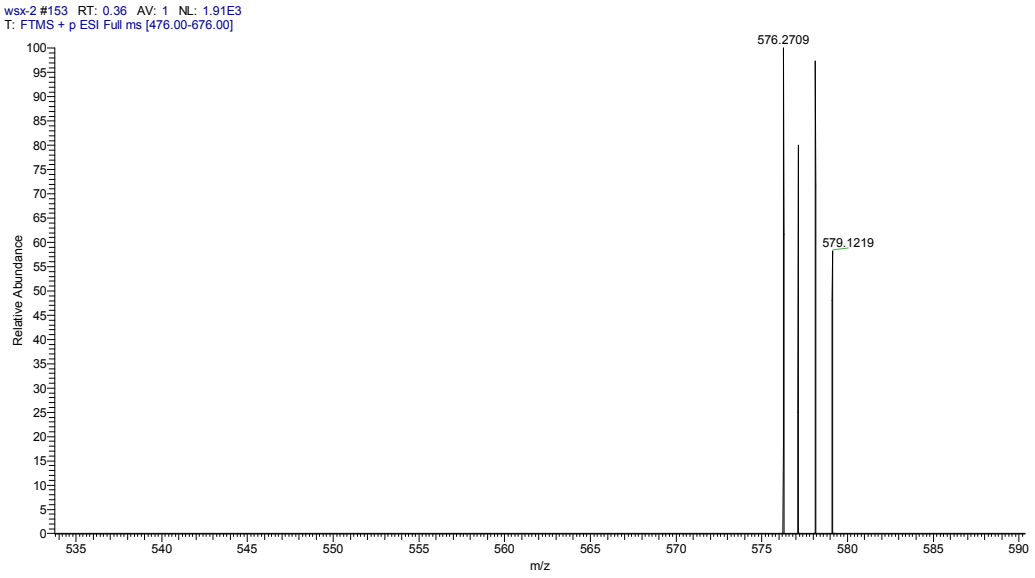

Figure S4 HRMS of NapPT-1

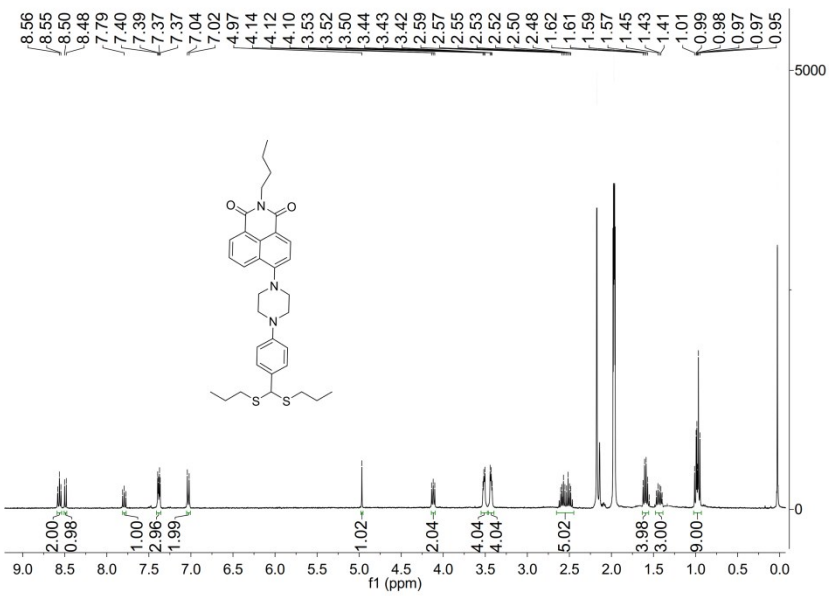

Figure S5 ^{1}H NMR spectrum of NapPT-1 in CD_3CN

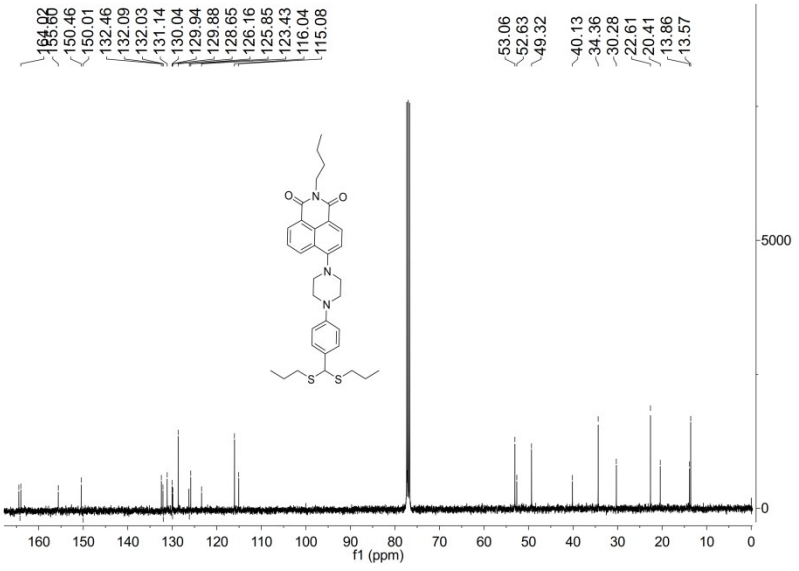

Figure S6 ^{13}C NMR spectrum of NapPT-1 in $CDCl_3$

Synthesis of sensor NapPT-2

The mixture of Compound 2 (200 mg, 0.45 mmol) and 1-methylthioethanethiol (51.6 mg, 0.675 mmol, 1.5 equiv.) in 20 mL dichloromethane were stirred at 0 °C under nitrogen atmosphere for 10 minutes. 0.04 mL boron trifluoride diethyl ether solution,

diluted with 1 mL dichloromethane, was added dropwise to the reaction solution. The reaction was continuously stirring for 1 h at the room temperature. Subsequently, the reaction solution was washed with 60 ml (3×20 mL) saturated sodium chloride solution, extracted with methylene chloride, and dried over anhydrous sodium sulfate. The crude product was purified by silica chromatography (PE : EtOAc = 10 : 1, v : v) to afford an yellow solid product (250.29 mg, a yield of 87%). ^{1}H NMR (400 MHz, $CDCl_3$) δ 8.63 (d, *J* = 6.5 Hz, 1H), 8.57 (d, *J* = 8.0 Hz, 1H), 8.48 (d, *J* = 8.4 Hz, 1H), 7.77 - 7.71 (m, 1H), 7.49 - 7.45 (m, 2H), 7.31 (s, 1H), 7.00 (d, *J* = 8.7 Hz, 2H), 5.35 (s, 1H), 4.23 - 4.17 (m, 2H), 3.53 (d, *J* = 4.3 Hz, 4H), 3.45 (d, *J* = 4.8 Hz, 4H), 2.15 (dd, *J* = 9.6, 7.1 Hz, 5H), 1.80 - 1.68 (m, 2H), 1.60 (s, 9H), 1.47 (dd, *J* = 15.1, 7.4 Hz, 2H). 1.00 (t, *J* = 7.3 Hz, 3H). ^{13}C NMR (100 MHz, $CDCl_3$) δ 164.41, 163.85, 155.56, 132.46, 131.14, 130.01, 129.89, 129.02, 126.27, 125.87, 116.06, 115.08, 53.05, 49.24, 47.51, 40.14, 30.28, 21.69, 20.40, 13.85. HRMS (ESI) calcd for $C_{33}H_{41}N_3O_2S_4$: 639.2082; found: 639.2098. $[M]^+$.

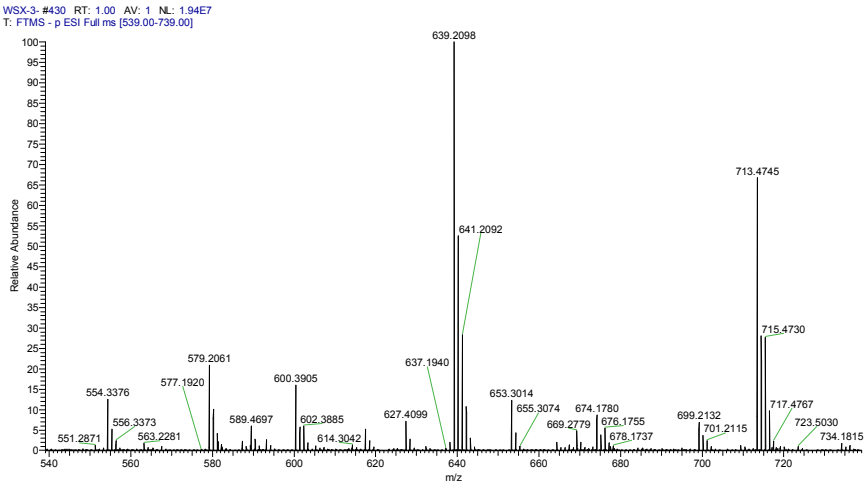

Figure S7 HRMS of NapPT-2

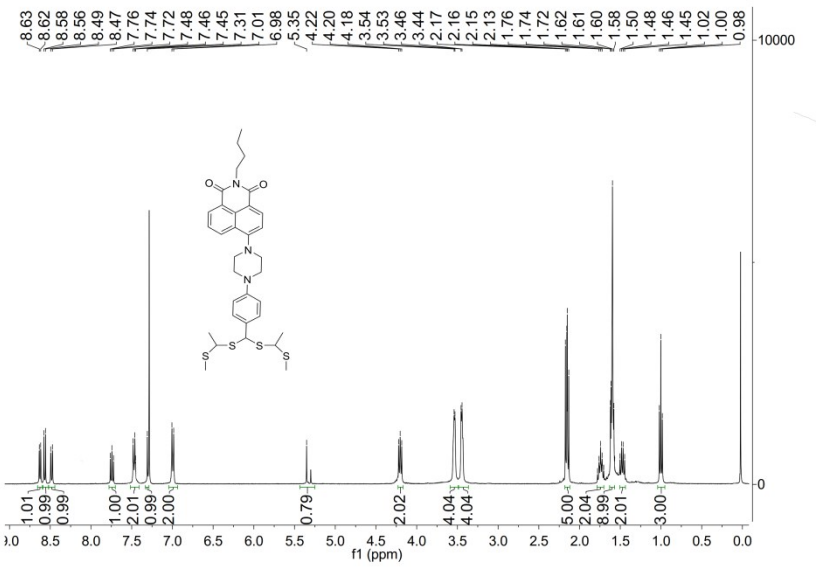

Figure S8 ^{1}H NMR spectrum of NapPT-2 in $CDCl_3$

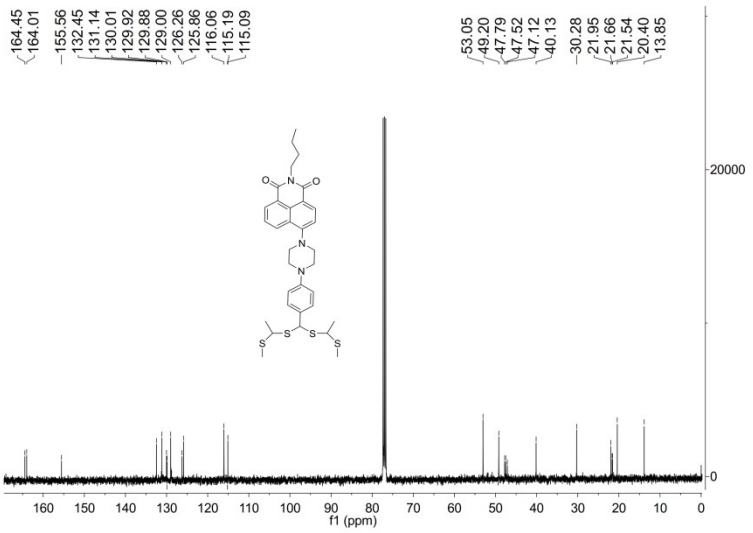

Figure S9 ^{13}C NMR spectrum of NapPT-2 in $CDCl_3$

2 Uv/visible absorption and fluorescene spectra of free sensors NapPT-1, NapPT-2 and compound 2

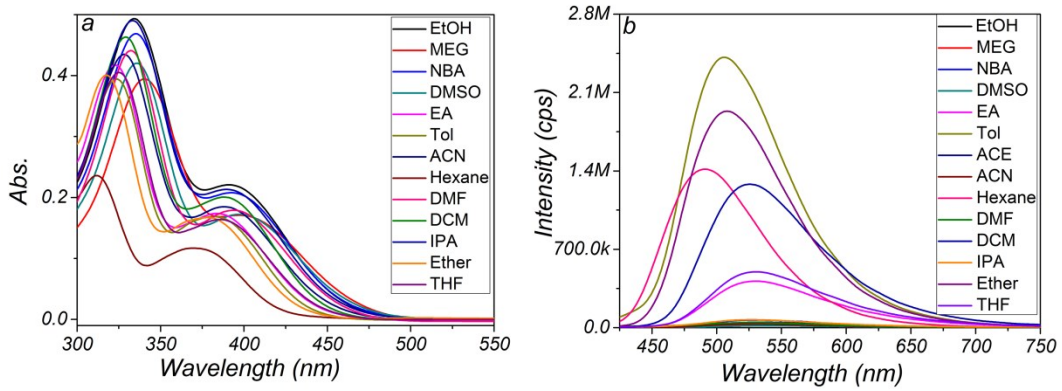

Figure S10 (a) UV/visible absorption spectra; (b) fluorescent spectra in all kinds of solutions of compound 2

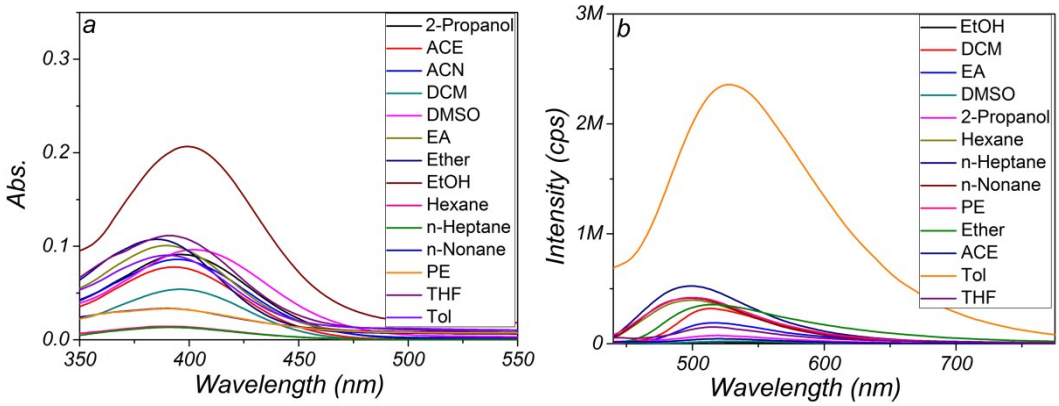

Figure S11 (a) UV/visible absorption spectra; (b) fluorescent spectra in all kinds of solutions of NapPT-1

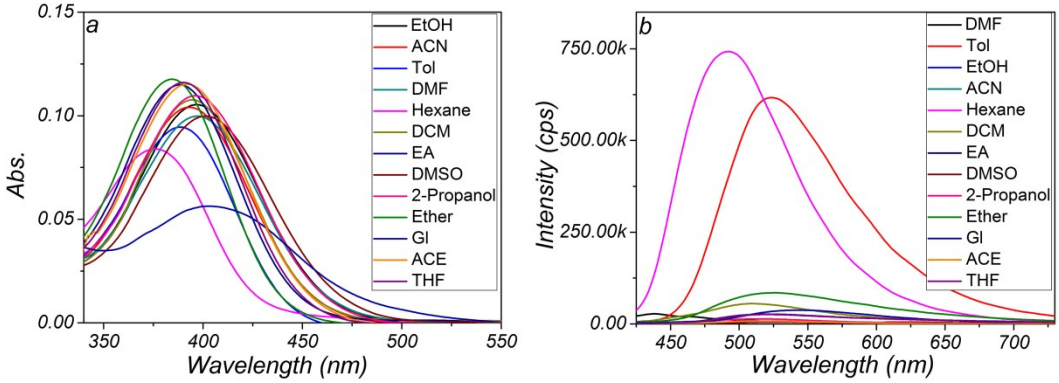

Figure S12 (a) UV/visible absorption spectra; (b) fluorescent spectra in all kinds of solutions of

NapPT-2

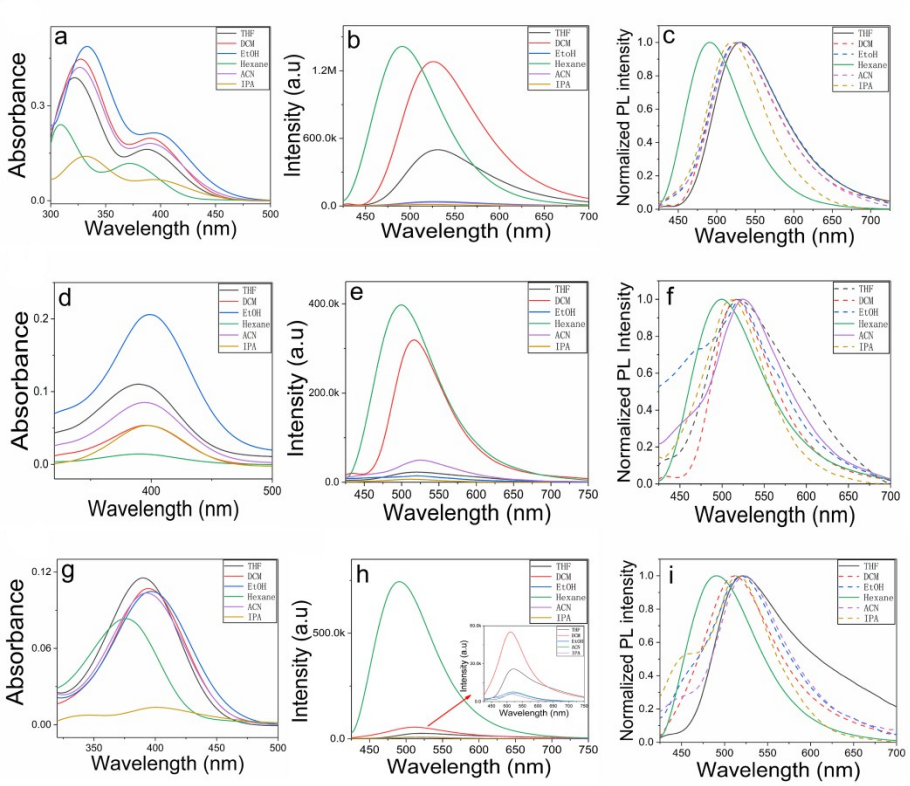

Figure S13 (a), (d) and (g) UV/visible absorption spectra; (b), (e) and (h) fluorescent spectra; (c), (f) and (i) normalized intensity of fluorescent spectra of compound 2, NapPT-1 and NapPT-2 in six solvents of different polarity (HEXANE: n-hexane; DCM: dichloromethane; THF: tetrahydrofuran; MeCN: acetonitrile; IPA: i-propanol; EtOH: ethanol)

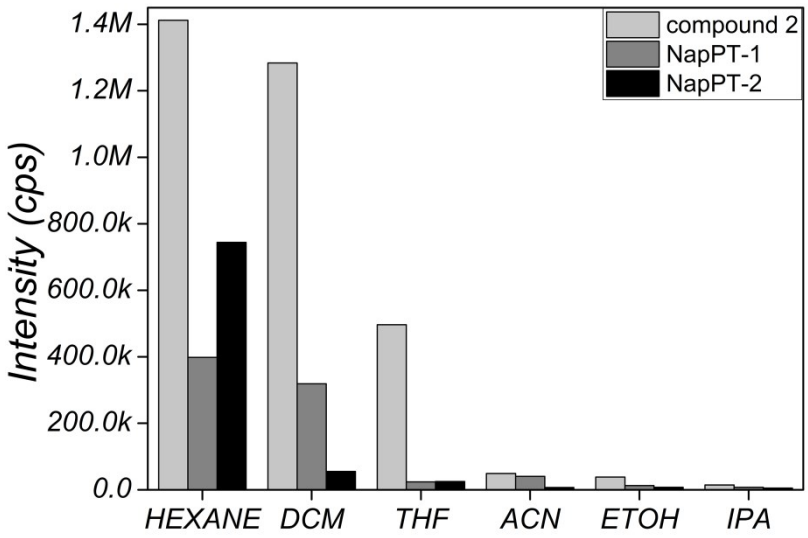

Figure S14 Fluorescent intensity of compound 2, NapPT-1 and NapPT-2 in six solvents of different polarity (HEXANE: n-hexane; DCM: dichloromethane; THF: tetrahydrofuran; MeCN: acetonitrile; IPA: i-propanol; EtOH: ethanol)

3 The spectra response of fluorescent sensor NapPT-2 and compound 2 over wide temperature range

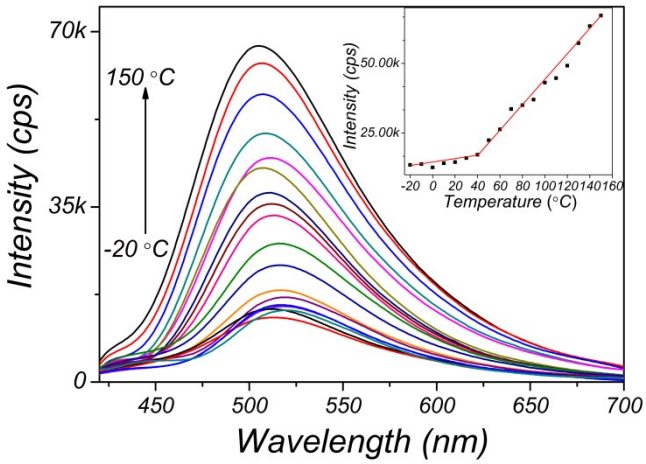

Figure S15 Fluorescent emission spectra of NapPT-2 in MOE (5.0×10^{-6} mol/L) recorded from -20 to 150 °C, Excitation wavelength: 400 nm.

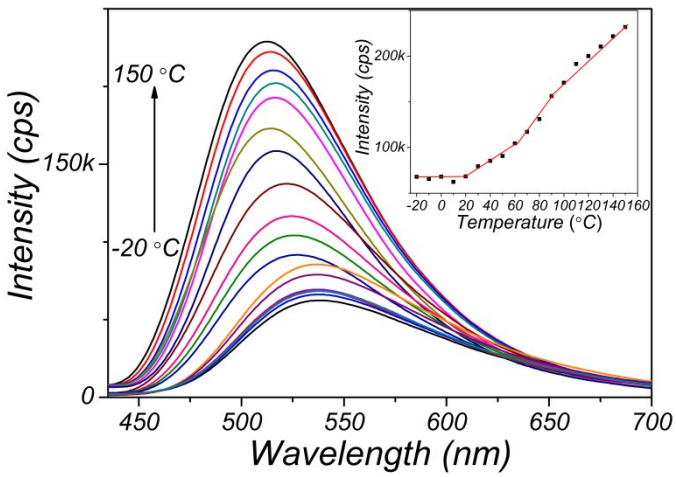

Figure S16 Fluorescent emission spectra of compound 2 in MOE (5.0×10^{-6} mol/L) recorded from -20 to 150 °C, Excitation wavelength: 400 nm.

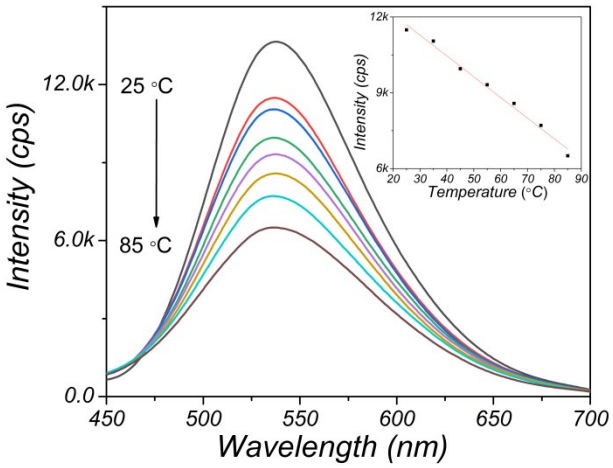

Figure S17 Fluorescent emission spectra of NapPT-2 in water (5.0×10^{-6} mol/L) recorded from 15 to 95 °C. Excitation wavelength: 400 nm.

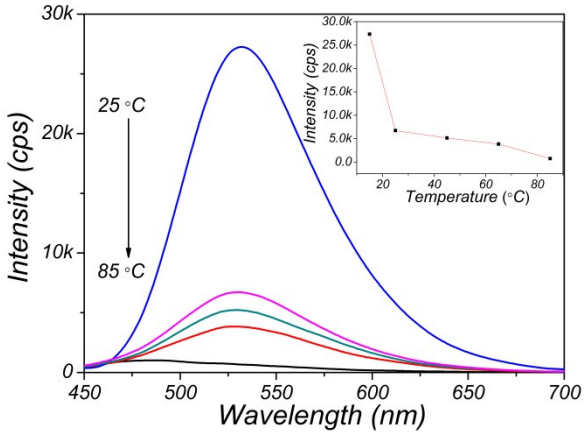

Figure S18 Fluorescent emission spectra of compound 2 in water (5.0×10^{-6} mol/L) recorded from 15 to 95 °C. Excitation wavelength: 400 nm.

4 The reversibility and stability of fluorescent sensor NapPT-2 in MOE and water

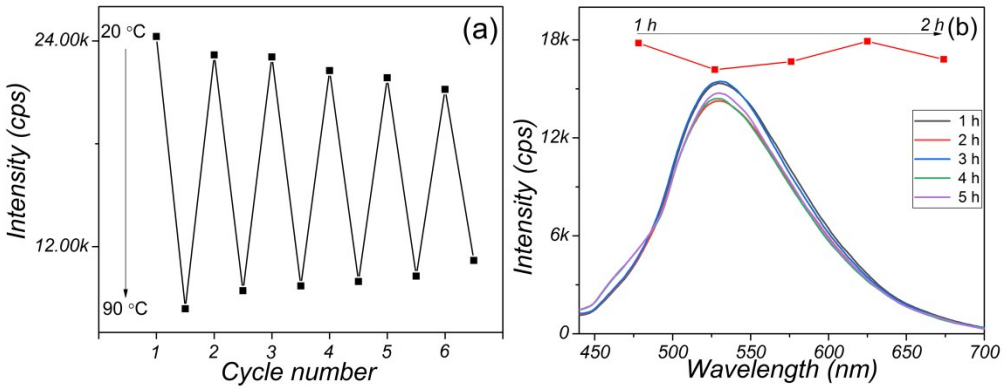

Fig. S19 (a) The fluorescent intensity of NapPT-1 (5.0×10^{-6} mol/L) upon cycling temperature from 20 to 100 °C in water. (b) The fluorescent intensity of NapPT-1 (5.0×10^{-6} mol/L) in water at 60 °C for 5 hours. All these measurements were carried out in ambient atmosphere.

5 The density functional theory of NapPT-2 and compound 2

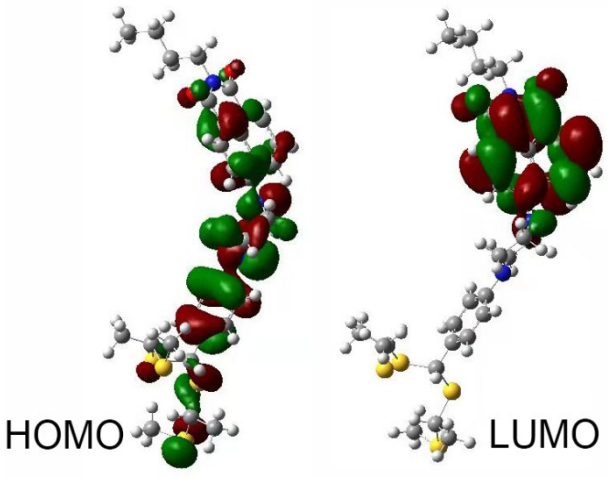

Figure S20 (a) HOMO and (b) LUMO of NapPT-2 by the density functional theory (DFT) calculations at b3lyp/6-311++g(2df,2p) level

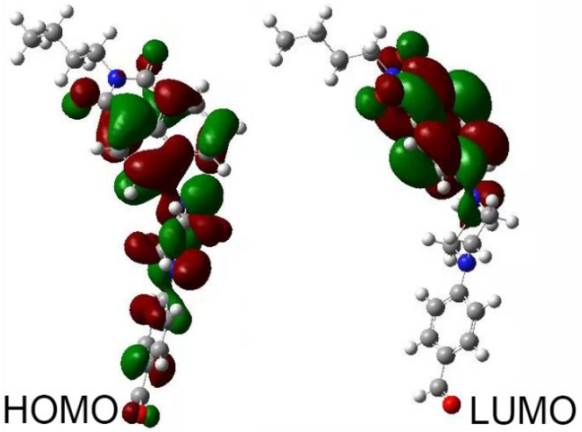

Figure S21 (a) HOMO and (b) LUMO of compound 2 by the density functional theory (DFT) calculations at b3lyp/6-311++g(2df,2p) level

6 Fluorescent quantum yield of compound 2, NapPT-1 and NapPT-2 in all kinds of solvents

Table S1 Fluorescent quantum yield of compound 2, NapPT-1 and NapPT-2 in all kinds of solvents

Compounds	Solvents	$\lambda_{Abs\ (nm)}$[a]	$\lambda_{Flu\ (nm)}$[b]	Φ_f[c]
Compound 2	water	390	525	0.022
	THF	395	520	0.051
	ACN	400	510	0.003
	EtOH	390	525	0.002
	DCM	390	495	0.153
	Hexane	395	575	0.015
	MOE	400	490	0.038
	MOE -heat	400	480	0.035
NapPT-1	water	400	515	0.019
	THF	400	525	0.004
	ACN	390	500	0.008
	EtOH	400	500	0.016
	DCM	400	515	0.040
	Hexane	400	525	0.038
	MOE	390	545	0.004
	MOE -heat	380	545	0.022
NapPT-2	water	400	125	0.005
	THF	400	525	0.014
	ACN	390	550	0.030
	EtOH	400	510	0.008
	DCM	400	490	0.057
	Hexane	400	545	0.049
	MOE	390	545	0.014
	MOE -heat	380	525	0.057

[a] The maximum absorption wavelength.

[b] The maximum fluorescent emission wavelength (λex= 400 nm).

[c] The fluorescence quantum yield measured by using fluorescein (Φ_f=0.95±0.03) as a standard.

7 The fluorescent thermometer performance parameters

Table S2 The fluorescent thermometer performance parameters

Compounds	Response type	λem (nm)	Working range (K/°C)	S_A [a]
NapPT-1	Off-On	500/525	253.15-423.15 K	0.0438 K^{-1}
$Y_{1.97}Ho_{0.03}O_3$/ $Mg_2Ti_{0.99}Mn_{0.01}O_4$	On-Off	550/650	RT-100 °C	4.6% $°C^{-1}$/ 5.1% $°C^{-1}$ [1]
FIPAC	Ratio	442/595	138-343 K	0.194 K^{-1} [2]
Benzothiadiazole-PNNPAM-BODIPY	Ratio	515/580	298-313 K	0.041 K^{-1} [3]
Triarylphosphine oxide	Ratio	380/480	223-373 K	0.012 K^{-1} [4]

BODIPY derivatives with OEG dendrons	On-Off	521	288-318 K	0.024 K^{-1} [5]
Mito thermo yellow	On-Off	564	283-343 K	0.025 K^{-1} [6]
BAI	On-Off	559	283-323 K	0.024 K^{-1} [7]
DB-TPE nanoparticles	On-Off	479	278-338 K	0.011 K^{-1} [8]
RhB, rhodamine110 labeled F127 polymers	Ratio	520/580	253-383 K	0.07 $6K^{-1}$ [9]
6-FAM	Ratio	515/575	273-373 K	0.07 K^{-1} [10]

[a] The thermal sensitivity：$S_A=\frac{1}{Xref}\times\frac{\Delta X}{\Delta T}$； （X：$\Phi_f$） [11]

References

1. M. Sekulić, V. Đorđević, Z. Ristić, M. Medić and M. D. Dramićanin, *Advanced Optical Materials*, 2018, **6**.
2. J. Chen, Y. Wu, X. Wang, Z. Yu, H. Tian, J. Yao and H. Fu, *Phys Chem Chem Phys*, 2015, **17**, 27658-27664.
3. S. Uchiyama, T. Tsuji, K. Ikado, A. Yoshida, K. Kawamoto, T. Hayashi and N. Inada, *Analyst*, 2015, **140**, 4498-4506.
4. Q. Fang, J. Li, S. Li, R. Duan, S. Wang, Y. Yi, X. Guo, Y. Qian, W. Huang and G. Yang, *Chem Commun (Camb)*, 2017, **53**, 5702-5705.
5. H. Wang, Y. Wu, Y. Shi, P. Tao, X. Fan, X. Su and G. C. Kuang, *Chemistry*, 2015, **21**, 3219-3223.
6. S. Arai, M. Suzuki, S. J. Park, J. S. Yoo, L. Wang, N. Y. Kang, H. H. Ha and Y. T. Chang, *Chem Commun (Camb)*, 2015, **51**, 8044-8047.
7. V. F. Pais, J. M. Lassaletta, R. Fernandez, H. S. El-Sheshtawy, A. Ros and U. Pischel, *Chemistry*, 2014, **20**, 7638-7645.
8. A. Ozawa, A. Shimizu, R. Nishiyabu and Y. Kubo, *Chem Commun (Camb)*, 2015, **51**, 118-121.
9. Y. Wu, J. Liu, J. Ma, Y. Liu, Y. Wang and D. Wu, *ACS Appl Mater Interfaces*, 2016, **8**, 14396-14405.
10. Y. Wu, J. Liu, Y. Wang, K. Li, L. Li, J. Xu and D. Wu, *ACS Appl Mater Interfaces*, 2017, **9**, 11073-11081.
11. C. Gota, S. Uchiyama, T. Yoshihara, S. Tobita and T. Ohwada, *Journal of Physical Chemistry B*, 2008, **112**, 2829-2836.